ACS OMEGA

Open Access

http://pubs.acs.org/journal/acsodf

Article

Germanium and Tin Precursors for Chalcogenide Materials Containing *N*-Alkoxy Thioamide Ligands

Heenang Choi, Young Eun Song, Dongseong Park, Chanwoo Park, Bo Keun Park, Seung Uk Son, Jongsun Lim, and Taek-Mo Chung*

Cite This: *ACS Omega* 2024, 9, 28707−28714

Read Online

ACCESS | Metrics & More | Article Recommendations | Supporting Information

ABSTRACT: This study describes the synthesis of germanium and tin complexes $Ge(mdpaS)_2$ (**1**), $Ge(edpaS)_2$ (**2**), $Ge(bdpaS)_2$ (**3**), $Ge(empaS)_2$ (**4**), $Sn(mdpaS)_2$ (**5**), $Sn(edpaS)_2$ (**6**), $Sn(bdpaS)_2$ (**7**), and $Sn(empaS)_2$ (**8**) (mdpaSH = (*Z*)-*N*-methoxy-2,2-dimethylpropanimidothioic acid; edpaSH = (*Z*)-*N*-ethoxy-2,2-dimethylpropanimidothioic acid; bdpaSH = (*Z*)-*N*-(tert-butoxy)-2,2-dimethylpropanimidothioic acid; empaSH = (*Z*)-*N*-ethoxy-2-methylpropanimidothioic acid), using newly designed *N*-alkoxy thioamide ligands as precursors for metal chalcogenide materials. All complexes were characterized using various analytical techniques, and the single-crystal structures of complexes **5** and **7** revealed a distorted seesaw geometry in the monomeric SnL_2 form. Thermogravimetric (TG) curves showed differences between Ge compounds, which exhibited single-step weight losses, and Sn compounds, which exhibited multistep weight losses. As a result, we suggest that the synthesized complexes **1**−**8** are potential precursors for group IV metal chalcogenide materials.

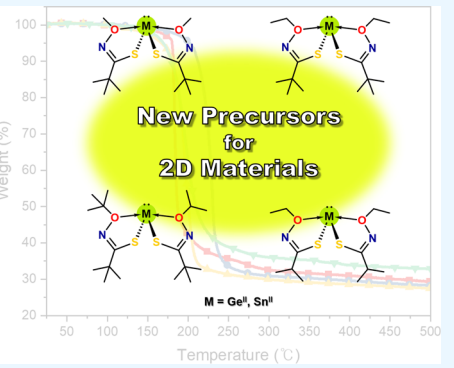

INTRODUCTION

In the modern electronics industry, layered materials are attractive components because they can be applied in a variety of optical fields such as transistors, photodetectors, ultrafast lasers, touch panels, and optical modulators.[1−4] Among layered materials, two-dimensional (2D) materials are very suitable for various electronic device fields because they have excellent electron mobility and a large surface area compared to zero-dimensional or one-dimensional materials.[5,6] Graphene is a representative 2D material; however, it has no band gap and weak light absorption, so its application in the optoelectronic field is limited; therefore, interest in the exploration of new layered materials is increasing.[7−12] Among many other 2D materials, tin and germanium monochalcogenide materials[13] (GeS,[14] GeSe,[15] SnS,[16−18] and SnSe[19,20]) have been discovered to have anisotropic structure, and they have recently gained attention and popularity in the semiconductor field due to their anisotropic electronic/optical properties, high absorption coefficient, high thermal stability, high oxidation resistance, structural stability, suitable band gap, and photoluminescence.[21] In addition, they are environmentally friendly, economical, and have low toxicity, making them attractive alternatives to toxic lead chalcogenides.[22,23]

GeS is a p-type semiconductor that is stacked together through van der Waals interactions and has a direct band gap of 1.65 eV[24] in the bulk visible region. In a single layer, it has an indirect band gap of 2.34 eV and an electron mobility of 3680 $cm^2/(V\ s)$.[25] Although GeS has not been studied in detail so far, it is a promising candidate material for batteries,[23,26,27] photovoltaics (PV), and light sensing owing to its excellent photosensitivity, convenient band gap in the visible region, and strong absorption over a wide spectral range and conductivity.[28,29]

SnS is essentially a p-type semiconductor[30,31] with a band gap of 0.9−1.8 eV,[32] a high absorption coefficient of over 10^4 cm^{-1},[33] a hole density of 10^{15}−10^{18} cm^{-3}, and a high mobility of ∼90 $cm^2/(V\ s)$. These properties make SnS a potential candidate for the development of low-cost thin-film solar cell absorbers[34] and sustainable photovoltaic (PV) absorbers.[35,36]

Various methods have been employed to form high-quality GeS and SnS materials, including sol−gel processes, solid-state reactions, solution processes, laser photolysis, electrodeposition, chemical vapor decomposition (CVD), and atomic layer deposition (ALD).[16,37−43]

In addition, single-source precursors provide several advantages: much easier handling, high atom efficiency, better homogeneity, and a simple delivery system with properties such as stoichiometry, morphology, and area selectivity of the target material as directly controlled in the precursor.[44−46] In the case of SnS, some precursors were examined as single sources without an H_2S reagent, such as Bz_3SnCl(saltscz)

Received: March 29, 2024
Revised: June 5, 2024
Accepted: June 7, 2024
Published: June 20, 2024

(saltscz = thiosemicarbazone of salicylaldehyde), Bz_3SnCl(4-clbenztscz) (4-clbenztscz = thiosemicarbamicarbazone of 4-chlorobenzaldehyde),[47] $Sn(^nBu)_2[S_2CN(RR')]_2$ (R, R′ = Et; R = Me and R′ = ^{n}Bu; R, R′ = ^{n}Bu; R = Me and R′ = nHex),[48] bis[2-methyl-*N*-(1-methylethyl)-propanethioamide]tin(II), bis[*N*-(1,1-dimethylethyl)-2-methylpropanethioamide]tin-(II),[49] (dimethylamido)(*N*-phenyl-*N*′,*N*′-dimethylthiouriate)-tin(II) dimer,[50] and {CyNC(NMe$_2$)NCy}-SnS.[51]

However, because only an extremely small number of single-source precursors for GeS materials have been previously reported, germanium chalcogenide materials are usually obtained from separate sources, such as germanium, germanium halides, and alkyl germanium with sulfur reagents.[26,44]

Therefore, we focused on developing new single-source precursors for germanium and tin sulfide materials, and synthesized newly designed organic ligands containing sulfur atoms, such as mdpaSH, edpaSH, bdpaSH, and empaSH, using previously reported ligands.[52,53]

Herein, we report the synthesis of new Ge and Sn complexes for use as chalcogenide materials and thin films as single-source precursors. Each molecule of the designed homoleptic compounds has one metal atom and two bidentate ligands containing two sulfur atoms. These complexes are designated as Ge(mdpaS)$_2$ (**1**), Ge(edpaS)$_2$ (**2**), Ge(bdpaS)$_2$ (**3**), Ge(empaS)$_2$ (**4**), Sn(mdpaS)$_2$ (**5**), Sn(edpaS)$_2$ (**6**), Sn(bdpaS)$_2$ (**7**), and Sn(empaS)$_2$ (**8**). Complexes **1**−**8** were characterized using nuclear magnetic resonance (NMR) spectroscopy, Fourier-transform infrared (FT-IR) spectroscopy, thermogravimetric analysis (TGA), and elemental analysis (EA). Complexes **5** and **7** were further characterized using single-crystal X-ray crystallography (SC-XRC).

RESULTS AND DISCUSSION

We designed a series of new ligands, *N*-alkoxy thioamides, which were synthesized by substituting an oxygen atom in previously reported *N*-alkoxy carboxamide ligands with a thiol group. The reaction between NH-form ligands (mdpaH, edpaH, bdpaH, and empaH)[52] and 0.25 equiv of P_2S_5 afforded the desired SH-form ligands (mdpaSH, edpaSH, bdpaSH, and empaSH) in moderate yields of 48−72% (Scheme 1).

Scheme 1. Synthetic Scheme of a Series of *N*-Alkoxy Thioamide Ligands

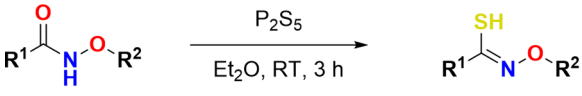

R^1 = ^{t}Bu, R^2 = Me; **mdpaSH**
R^1 = ^{t}Bu, R^2 = Et; **edpaSH**
R^1 = ^{t}Bu, R^2 = ^{t}Bu; **bdpaSH**
R^1 = ^{i}Pr, R^2 = Et; **empaSH**

The four newly synthesized ligands were characterized using physicochemical analysis and reacted to obtain the desired Ge and Sn complexes. All of the complexes in this study were successfully synthesized via an acid−base reaction with germanium or tin bis(trimethylsilyl)amide and the respective *N*-alkoxy thioamide ligands in a ratio of 1:2, as shown in Scheme 2.

Complexes **1**-**8** were obtained as white powders by recrystallization and further purified under each condition, as described in the Experimental Section.

The ^{1}H NMR spectra demonstrated that all peaks of **1**−**8** were fully shifted relative to the respective corresponding free ligands. The SH peak and btsa peak in the complexes **1**−**8** were noticeably absent.[54] Compound **1** showed two singlets at δ_H = 1.33 (18H, *tert*-butyl group) and 3.85 (6H, *O*-methyl group) ppm. The ^{1}H NMR spectrum of **2** displayed one triplet at δ_H = 1.33 (6H, CH_3 of *O*-ethyl group) ppm, one singlet at δ_H = 1.37 (18H, *tert*-butyl group) ppm, and a quartet at δ_H = 4.23 (4H, CH_2 of *O*-ethyl group) ppm. The spectrum of **3** exhibited only the *tert*-butyl group as two singlets of 18H at δ_H = 1.39 and 1.47 ppm. The spectrum for complex **4** contains one doublet at δ_H = 1.26 (12H, CH_3 of isopropyl group) ppm, one triplet at δ_H = 1.30 (6H, CH_3 of *O*-ethyl group) ppm, one septet at δ_H = 2.84 (2H, C*H* of isopropyl group) ppm, and one quartet at δ_H = 4.23 (4H, CH_2 of *O*-ethyl group) ppm. Likewise, ^{1}H NMR spectra of tin complexes **5**−**8** containing the corresponding ligands showed the same patterns as the germanium complexes. (Figures S1−S16).

Additionally, the S−H stretching frequency of free ligands and the Si−CH_3 rocking vibration from bis(trimethylsilyl)-amide disappeared in the FT-IR spectra of the germanium and tin products. On the other hand, the C−H stretching from alkane groups was exhibited in the range of ν = 2963−3109 cm^{-1}.[55]

To investigate the molecular structure of the solid-phase conformer using X-ray crystallography (XRC), single crystals were grown in a saturated toluene solution at room temperature in an Ar-filled glovebox. Complexes **5** and **7** have a triclinic crystal system in the space group *P*-1 and exist as monomers with two molecules in each unit cell.

The crystal structures of **5** and **7** reveal a distorted seesaw geometry with one Sn atom bonded to two respective corresponding ligands such as mdpaS (**5**) and bdpaS (**7**), and they form two κ^2-*O*,*S*-chelating structures with five-membered ring metallacycles, as shown in Figures 1 and 2. The lone pair of Sn (II) atoms is located at one equatorial position, similar to the trigonal bipyramidal geometry, and repulsion from the lone pair results in a butterfly shape. The two O atoms, O1 and O2, in each ligand occupy the axial position, whereas the two S atoms (S1 and S2) are located in the equatorial plane with a lone pair.

In the case of complex **5**, the bond distance Sn−S1 is 2.5368(11) Å and Sn−S2 is 2.5345(10) Å. The O1−Sn−O2 axial angle and S1−Sn−S2 equatorial angle with mdpaS ligands were found to be 143.45(9) and 97.03(4)°, respectively, and the bite angles are 71.76(7)° (S1−Sn−O1) and 71.41(7)° (S2−Sn−O2). For **7**, the Sn−S1 bond distance is 2.5161(4) Å, and Sn−S2 is 2.5455(4) Å. The axial direction O1−Sn−O2 has an angle of 146.95(3)°, and that in the equatorial direction is 95.574(15)°. The bite angles for the bdpaS ligands are 72.98(3)° and 70.63(3). These results demonstrate that the respective bond distances of Sn−S are within the range of reported distance (2.510−2.822 Å),[56] and compound **7**, which has two bdpaS ligands containing a *tert*-butyl group, has a more clearly tilted structure than that of **5**. The reason for the differences in the distances or angles, even within a series of similar ligands, could be the replacement of relatively sterically compact functional groups, such as methyl, by bulkier *tert*-butyl groups of the bdpaS ligand (Table 1).

https://doi.org/10.1021/acsomega.4c03019
ACS Omega 2024, 9, 28707−28714

Scheme 2. Synthetic Scheme of Complexes 1−8

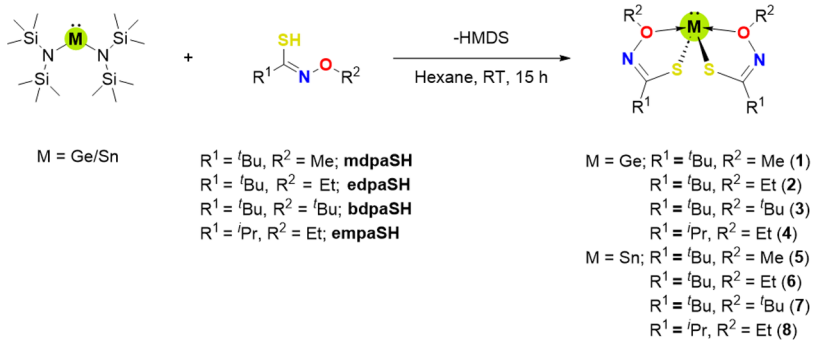

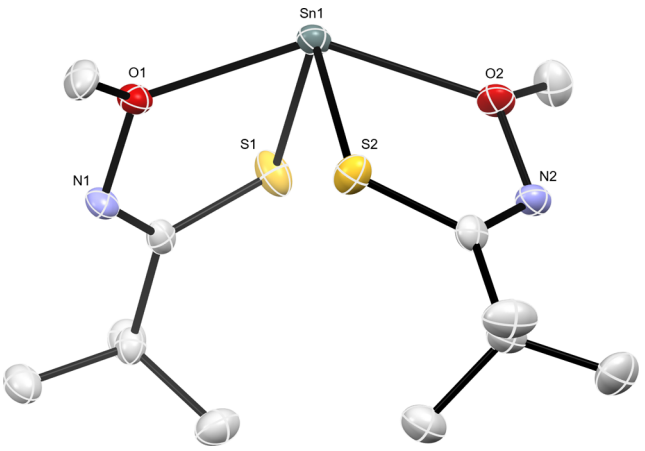

Figure 1. Molecular structure of complex **5**. All hydrogen atoms are omitted for clarity (green, tin; red, oxygen; blue, nitrogen; gray, carbon).

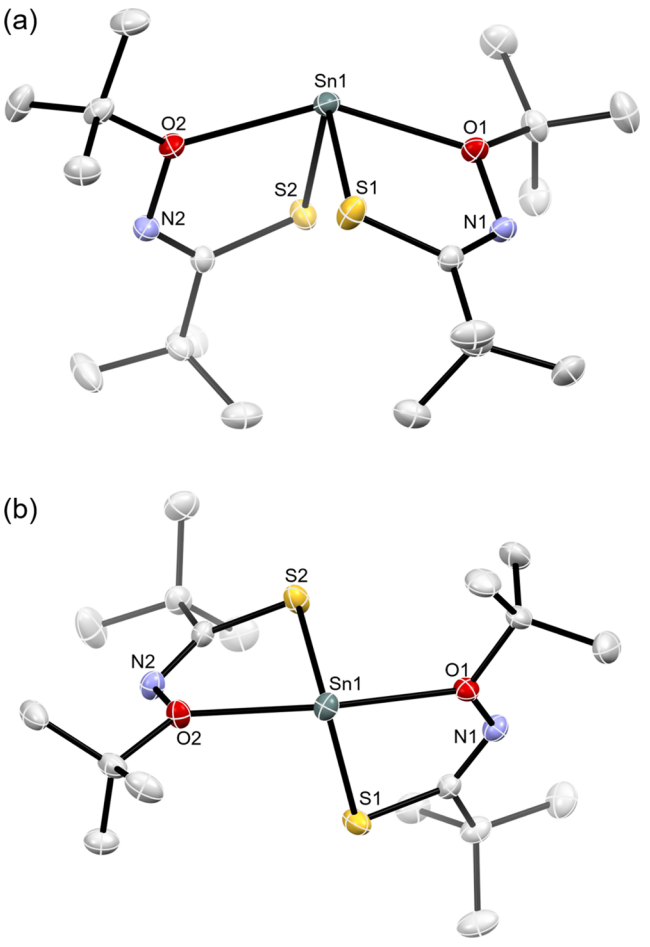

Figure 2. (a) Side view and (b) top view of molecular structure of complex **7**. All hydrogen atoms are omitted for clarity (green, tin; red, oxygen; blue, nitrogen; gray, carbon).

The melting points of complexes **3** and **7**, which contain the *tert*-butyl group, were relatively high compared to those of compounds **4** and **8**, which contain the empaS ligand. Among them, the melting points of the germanium complexes **1**−**3** are 165, 129, and 194 °C, respectively, which are higher than those of the tin complexes **5**−**7**, 90, 61, and 98 °C, respectively.

Thermogravimetric (TG) analysis of all complexes was performed from 30 to 500 °C at a heating rate of 20 K/min. Germanium complexes **1**−**4** showed single-step TG curves. The weight loss of each compound started at 139, 156, 125, and 138 °C, respectively. Among these, **2** showed the highest thermal stability as shown by the high decomposition temperature, and **3** had the lowest residue of 27% with the nonvolatile residue measured at 500 °C. In contrast, tin complexes **5**−**8** exhibited multistep weight loss. The 1% onset temperatures were confirmed at 126, 114, 127, and 126 °C, respectively, and the lowest amount of nonvolatile residue at 500 °C was 34% in the case of compound **7**. The residues of all of the complexes depended on the type of ligand. Compounds **4** and **8** with the empaS ligand showed the highest residual weight, followed by **1** and **5** with mdpaS, **2** and **6** with edpaS, and **3** and **7** with bdpaS ligands, which showed the lowest residual weight.

The differential scanning calorimetry (DSC) diagrams of the complexes feature an endothermic peak at 160 (**1**), 130 (**2**), 199 (**3**), 88 (**4**), 92 (**5**), 61 (**6**), 102 (**7**), 80 (**8**) °C, and this is attributed to the differences in melting point of each corresponding compound. In addition, the exothermic peak can be regarded as the decomposition temperature of the specific materials, as seen in their TGA behavior (Figures 3 and 4, Table 2).

EXPERIMENTAL SECTION

General Remarks. ^{1}H and $^{13}C\{1H\}$ NMR spectra were recorded using Bruker 400 and 500 MHz spectrometers with benzene-d_6 as the solvent and reference. FT-IR spectra were collected in the range 4000−400 cm^{-1} using a Nicolet Nexus FT-IR spectrophotometer with a 4 mm KBr window of KBr pellets. The melting points of the samples were measured using closed-ended capillaries in an electrothermal melting point apparatus, and were not corrected. The TGA was conducted at

https://doi.org/10.1021/acsomega.4c03019
ACS Omega 2024, 9, 28707−28714

Table 1. Selected Bond Lengths (Å) and Bond Angles (deg) for Complex 5 and 7

	Complex	
Bond Length (Å)	5	7
Sn−O1	2.377(3)	2.4001(10)
Sn−O2	2.415(3)	2.4830(11)
Sn−S1	2.5368(11)	2.5161(4)
Sn−S2	2.5345(10)	2.5455(4)
	Complex	
Bond Angles (deg)	5	7
O1−Sn−S1	71.76(7)	72.98(3)
O1−Sn−S2	83.71(7)	83.37(3)
O2−Sn−S1	84.87(7)	89.21(3)
O2−Sn−S2	71.41(7)	70.63(3)
O1−Sn−O2	143.45(9)	146.95(3)
S1−Sn−S2	97.03(4)	95.574(15)

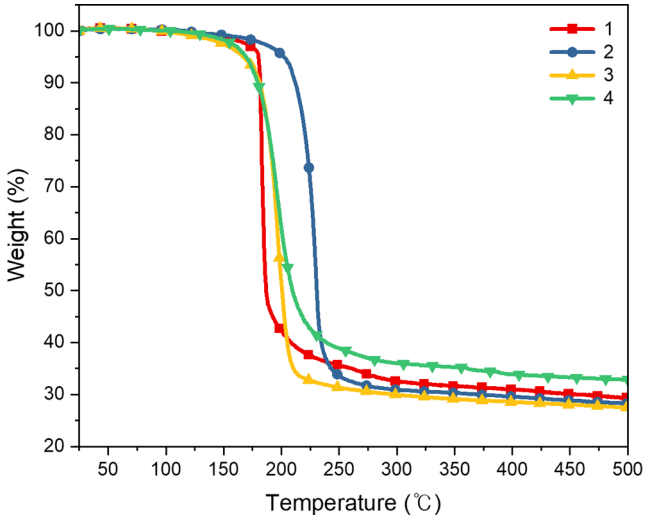

Figure 3. TGA curves of germanium complexes **1**−**4**.

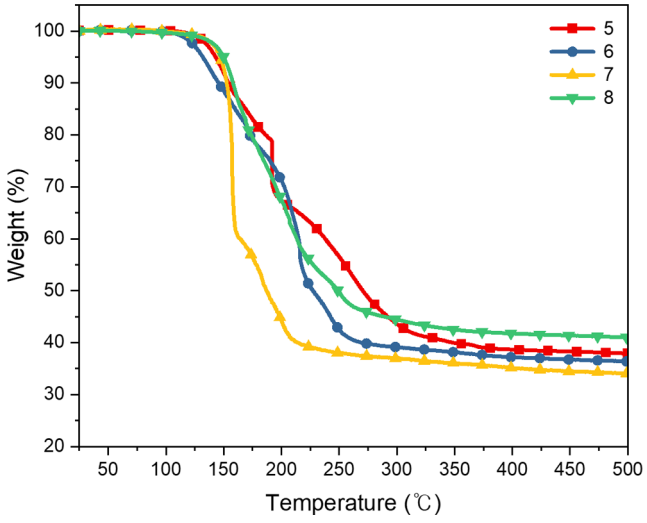

Figure 4. TGA curves of tin complexes **5**−**8**.

a scan rate of 20 K/min using a NETZSCH TG 209 F3TG instrument under N_2 gas in a glovebox. EA was performed using a Thermo Scientific Flash 2000 organic elemental analyzer. Commercial chemicals were purchased from Aldrich, TCI, Alfa Aesar, or STREM without further purification. All solvents were purified using an Innovative Technology PS-MD-4 solvent purification system, and all reactions were performed under inert, dry conditions in an Ar-filled glovebox. Ge(II) and Sn(II) amides, $Sn[N(SiMe_3)_2]_2$ and $Ge[N(SiMe_3)_2]_2$, were prepared according to literature procedures.[57,58] The applied *N*-alkoxy carboxamide ligands, mdpaH, edpaH, and empaH, were prepared according to ref 52. The bdpaH ligand was synthesized following the same procedure, with O-*tert*-butylhydroxylamine hydrochloride used as a reagent to substitute the chlorine.

General Procedure for Synthesis of *N*-Alkoxy Thioamide Ligands. P_2S_5 (0.25 equiv) was slowly added to a diethyl ether solution containing the *N*-alkoxy carboxamide ligands mdpaH, edpaH, bdpaH, or empaH. The reaction mixture was stirred under inert conditions in an Ar-filled glovebox at room temperature. A white powder was gradually produced with constant stirring. After 3 h, the mixture was filtered to remove the solids, and the filter cake was washed three times with diethyl ether. The solvent was evaporated *in vacuo* using a pump at a pressure of approximately 120 Torr. Subsequently, the crude product was purified by distillation at 40 °C and collected in a cooling bath containing dry ice and ethanol to obtain the desired product as a colorless liquid. The synthesized ligands are very volatile and unstable at high temperatures. So, we purified the ligands in the conditions of low temperatures of 35−40 °C under 3 Torr, with a cooling bath to prevent the decomposition of ligands.

Synthetic Procedures. *mdpaSH.* mdpaH (10 g, 97.0 mmol) was used. Yield: 7.3 g (63%). ^{1}H NMR (500 MHz, C_6D_6) δ (ppm): 4.72 (s, 1H), 3.72 (s, 3H), 1.15 (s, 9H). ^{13}C NMR (126 MHz, C_6D_6) δ (ppm): 157.67, 61.50, 38.80, 28.82. FT-IR (KBr, cm^{-1}): 2968 (s), 2937 (m), 2901 (m), 2869 (w), 2817 (w), 2576 (w), 1741 (w), 1573 (m), 1477 (m), 1460 (m), 1394 (w), 1365 (m), 1242 (w), 1205 (w), 1086 (s), 1069 (m), 1036 (s), 1008 (s), 900 (m), 862 (w), 765 (m), 675 (w), 545 (m).

edpaSH. edpaH (10 g, 68.9 mmol) was used. Yield: 8.0 g (72%). ^{1}H NMR (400 MHz, C_6D_6) δ (ppm): 4.79 (s, 1H), 4.07 (q, J = 7.0 Hz, 2H), 1.16 (s, 8H), 1.10 (t, J = 7.1 Hz, 3H). ^{13}C NMR (126 MHz, C_6D_6) δ (ppm): 157.21, 157.20, 69.65, 38.88, 28.90, 14.73. FT-IR (KBr, cm^{-1}): 2970 (m), 2933 (m), 2900 (w), 2576 (w), 1575 (m), 1478 (m), 1461 (m), 1384 (m), 1365 (m), 1137 (w), 1092 (m), 1071 (m), 1037 (s), 1019 (s), 952 (s), 924 (s), 879 (w), 863 (w), 799 (w), 786 (w), 665 (w), 557 (w).

bdpaSH. bdpaH (10 g, 57.7 mmol) was used. Yield: 6.1 g (56%). ^{1}H NMR (500 MHz, C_6D_6) δ (ppm): 4.80 (s, 1H), 1.24 (s, 9H), 1.15 (s, 9H). ^{13}C NMR (101 MHz, C_6D_6) δ (ppm): 155.68, 79.44, 39.16, 28.98, 27.83. FT-IR (KBr, cm^{-1}): 2971 (s), 2932 (m), 2870 (w), 2573 (w), 1579 (m), 1476 (m), 1460 (m), 1386 (w), 1364 (s), 1238 (w), 1192 (s), 1072 (m), 1027 (m), 948 (s), 919 (s), 885 (m), 802 (m), 657 (w), 552 (m).

empaSH. empaH (10 g, 76.2 mmol) was used. Yield: 5.4 g (48%). ^{1}H NMR (400 MHz, C_6D_6) δ (ppm): 4.24 (s, 1H), 4.09 (q, J = 7.0 Hz, 2H), 2.52 (hept, J = 6.9 Hz, 1H), 1.11 (t, J = 7.0 Hz, 3H), 1.04 (d, J = 6.9 Hz, 6H). ^{13}C NMR (101 MHz, C_6D_6) δ (ppm): 154.54, 69.65, 36.12, 20.91, 14.74. FT-IR (KBr, cm^{-1}): 2968 (s), 2935 (m), 2879 (m), 2575 (w), 1650 (s), 1522 (m), 1471 (w), 1455 (w), 1383 (m), 1238 (m), 1154 (w), 1120 (m), 1099 (m), 1048 (s), 1016 (m), 948 (m), 882 (m), 851 (w), 684 (m), 647 (m), 560 (m).

https://doi.org/10.1021/acsomega.4c03019
ACS Omega 2024, 9, 28707−28714

Table 2. Thermal Physical Profiles of Complexes 1−8

Complex	Molecular Weight (g/mol)	Melting Point (°C)	Temperature at 1 wt % Loss (°C)	Temperature at 50 wt % Loss (°C)	Residual Mass (%)
1	365.09	165	139	187	29.4
2	393.14	129	156	231	28.2
3	449.25	194	125	200	27.5
4	365.09	86	138	210	32.8
5	411.17	90	127	249	37.9
6	439.22	61	114	227	36.4
7	495.33	98	128	187	34.0
8	411.17	85	126	270	41.0

General Procedure for Synthesis of Ge or Sn(*N*-alkoxy thioamide)$_2$. A hexane solution of *N*-alkoxy thioamide ligands (2 equiv), mdpaSH, edpaSH, bdpaSH, or empaSH was added dropwise to a hexane solution containing Ge(btsa)$_2$ or Sn(btsa)$_2$ (1 equiv). The reaction mixture was stirred continuously at room temperature in an Ar-filled glovebox for 15 h. Subsequently, the volatiles were evaporated *in vacuo*, and the crude pale yellow product was purified by recrystallization or sublimation to obtain the desired product as a white powder. X-ray-quality single crystals were grown from a saturated solution in toluene at room temperature in an Ar-filled glovebox by slow evaporation of the solvent.

Synthetic Procedures. *Ge(mdpaS)$_2$ (**1**).* mdpaSH (0.74 g, 5.0 mmol) was used for *N*-alkoxy thioamide ligand. The product was obtained by sublimation (140 °C, 0.3 Torr). Yield: 0.78 g (86%). M.P.: 165 °C. ^{1}H NMR (500 MHz, C_6D_6) δ (ppm): 3.85 (s, 6H), 1.33 (s, 18H). ^{13}C NMR (101 MHz, C_6D_6) δ (ppm): 158.0, 61.7, 40.1, 29.0. Anal. Found (Calcd for $C_{12}H_{24}N_2O_2S_2Ge$): C, 39.16 (39.48); H, 6.58 (6.63); N, 7.62 (7.67); S, 17.59 (17.57). FT-IR (KBr, cm^{-1}): 2981 (s), 2968 (s), 2937 (s), 2898 (m), 2865 (m), 2818 (w), 1568 (m), 1475 (m), 1456 (m), 1391 (w), 1362 (m), 1255 (w), 1068 (s), 1031 (s), 982 (s), 894 (m), 844 (w), 800 (m), 687 (m), 548 (w).

*Ge(edpaS)$_2$ (**2**).* edpaSH (0.81 g, 5.0 mmol) was used for *N*-alkoxy thioamide ligand. The product was obtained by sublimation (100 °C, 0.3 Torr). Yield: 0.9 g (92%). M.P.: 129 °C. ^{1}H NMR (500 MHz, C_6D_6) δ (ppm): 4.23 (q, J = 7.0 Hz, 4H), 1.37 (s, 18H), 1.31 (t, J = 7.0 Hz, 6H). ^{13}C NMR (101 MHz, C_6D_6) δ (ppm): 157.1, 70.4, 40.3, 29.1, 15.2. Anal. Found (Calcd for $C_{14}H_{28}N_2O_2S_2Ge$): C, 42.51 (42.77); H, 6.92 (7.18); N, 7.02 (7.13); S, 16.25 (16.31). FT-IR (KBr, cm^{-1}): 2970 (s), 2943 (m), 2928 (m), 2897 (w), 2868 (w), 1574 (m), 1474 (m), 1456 (m), 1440 (w), 1394 (w), 1377 (m), 1363 (m), 1091 (m), 1067 (s), 1033 (s), 994 (s), 936 (s), 925 (s), 873 (w), 789 (w) 691 (w).

*Ge(bdpaS)$_2$ (**3**).* bdpaSH (0.95 g, 5.0 mmol) was used for *N*-alkoxy thioamide ligand. The product was obtained by sublimation (90 °C, 0.3 Torr). Yield: 1.04 g (93%). M.P.: 194 °C. ^{1}H NMR (500 MHz, C_6D_6) δ (ppm): 1.47 (s, 9H), 1.39 (s, 9H). ^{13}C NMR (126 MHz, C_6D_6) δ (ppm): 152.4, 82.7, 41.1, 29.3, 28.4. Anal. Found (Calcd for $C_{18}H_{36}N_2O_2S_2Ge$): C, 47.95 (48.12); H, 8.19 (8.08); N, 6.08 (6.24); S, 14.55 (14.27). FT-IR (KBr, cm^{-1}): 2971 (s), 2928 (s), 2902 (m), 2866 (m), 1590 (m), 1474 (m), 1456 (m), 1389 (m), 1364 (s), 1264 (w), 1250 (w), 1188 (s), 1047 (m), 1010 (s), 951 (s), 916 (m), 873 (m), 861 (s), 806 (w), 765 (m).

*Ge(empaS)$_2$ (**4**).* empaSH (0.74 g, 5.0 mmol) was used for *N*-alkoxy thioamide ligand. The product was obtained by sublimation (140 °C, 0.3 Torr). Yield: 0.75 g (82%). M.P.: 86 °C. Sublimation: 105 °C/0.3 Torr. ^{1}H NMR (500 MHz, C_6D_6) δ (ppm): 4.23 (q, J = 7.0 Hz, 4H), 2.84 (h, J = 6.7 Hz, 2H), 1.30 (t, J = 7.1 Hz, 6H), 1.26 (d, J = 6.7 Hz, 12H). ^{13}C NMR (101 MHz, C_6D_6) δ (ppm): 154.4, 70.4, 37.1, 21.0, 15.2. Anal. Found (Calcd for $C_{12}H_{24}N_2O_2S_2Ge$): C, 39.87 (39.48); H, 6.49 (6.63); N, 7.25 (7.67); S, 17.42 (17.57). FT-IR (KBr, cm^{-1}): 2968 (s), 2930 (s), 2869 (m), 1580 (m), 1461 (m), 1381 (m), 1363 (w), 1309 (w), 1199 (w), 1148 (w), 1090 (m), 1052 (s), 996 (s), 950 (m), 921 (s), 846 (m), 701 (w), 678 (w).

*Sn(mdpaS)$_2$ (**5**).* mdpaSH (1.5 g, 10.0 mmol.) was used for *N*-alkoxy thioamide ligand. The white powder product was obtained by sublimation (100 °C, 0.3 Torr). Crystal was colorless. Yield: 1.87 g (91%). M.P.: 90 °C. ^{1}H NMR (500 MHz, C_6D_6) δ (ppm): 3.62 (s, 6H), 1.42 (s, 18H). ^{13}C NMR (126 MHz, C_6D_6) δ (ppm): 171.2, 61.6, 39.8, 30.2. Anal. Found (Calcd for $C_{12}H_{24}N_2O_2S_2Sn$): C, 34.94 (35.05); H, 5.85 (5.88); N, 6.82 (6.81); S, 15.62 (15.60). HR-MS: $[M]^+$ Found (Calcd for $C_{12}H_{24}N_2O_2S_2Sn$): 412.0302 (412.0301). FT-IR (ATR, cm^{-1}): 2969 (s), 2958 (s), 2940 (m), 2926 (m), 2900 (m), 2863 (m), 2820 (w), 1549 (s), 1480 (m), 1457 (m), 1424 (w), 1391 (m), 1363 (m), 1358 (m), 1249 (w), 1206 (w), 1188 (w), 1149 (w), 1061 (s), 1026 (s), 974 (s), 932 (w), 842 (s), 794 (s), 696 (m), 546 (m), 447 (w).

*Sn(edpaS)$_2$ (**6**).* edpaSH (1.6 g, 10.0 mmol.) was used for *N*-alkoxy thioamide ligand. The white powder product was obtained by sublimation (110 °C, 0.3 Torr). Yield: 2.11 g (96%). M.P.: 61 °C. Sublimation: 110 °C/0.3 Torr. ^{1}H NMR (500 MHz, C_6D_6) δ (ppm): 4.08 (q, J = 7.1 Hz, 2H), 1.44 (s, 9H), 1.12 (t, J = 7.0 Hz, 3H). ^{13}C NMR (126 MHz, C_6D_6) δ (ppm): 170.4, 71.4, 40.1, 30.3, 15.9. Anal. Found (Calcd for $C_{14}H_{28}N_2O_2S_2Sn$): C, 38.19 (38.28); H, 6.40 (6.43); N, 6.43 (6.38); S, 14.65 (14.60). HR-MS: $[M]^+$ Found (Calcd for $C_{14}H_{28}N_2O_2S_2Sn$): 440.0640 (440.0614). FT-IR (ATR, cm^{-1}): 2971 (s), 2927 (m), 2898 (m), 2865 (w), 1544 (m), 1480 (m), 1457 (m), 1437 (w), 1385 (m), 1362 (m), 1294 (w), 1248 (w), 1206 (w), 1167 (w), 1092 (m), 1062 (s), 1030 (s), 992 (s), 936 (s), 887 (s), 849 (s), 811 (w), 780 (m), 689 (m), 545 (m), 484 (m).

*Sn(bdpaS)$_2$ (**7**).* bdpaSH (1.9 g, 10.0 mmol.) was used for *N*-alkoxy thioamide ligand. The white powder product was obtained by sublimation (90 °C, 0.3 Torr). Crystal was colorless. Yield: 2.28 g (92%). M.P.: 98 °C. ^{1}H NMR (500 MHz, C_6D_6) δ (ppm): 1.42 (s, 18H), 1.37 (s, 18H). ^{13}C NMR (126 MHz, C_6D_6) δ (ppm): 167.4, 85.7, 40.6, 30.2, 29.3. Anal. Found (Calcd for $C_{18}H_{36}N_2O_2S_2Sn$): C, 43.40 (43.65); H, 7.36 (7.33); N, 5.63 (5.66); S, 12.65 (12.95). HR-MS: $[M]^+$ Found (Calcd for $C_{14}H_{28}N_2O_2S_2Sn$): 496.1219 (496.1240). FT-IR (ATR, cm^{-1}): 2973 (s), 2927 (m), 2900 (m), 2864 (m), 1559 (m), 1476 (m), 1456 (m), 1388 (m), 1362 (s), 1264 (w), 1242 (w), 1216 (w), 1173 (s), 1049 (s), 1034 (w),

https://doi.org/10.1021/acsomega.4c03019
ACS Omega 2024, 9, 28707−28714

1011 (m), 924 (m), 862 (s), 807 (m), 774 (m), 671 (m), 555 (m).

*Sn(empaS)$_2$ (**8**).* empaSH (1.5 g, 10.0 mmol.) was used for *N*-alkoxy thioamide ligand. The colorless liquid product was obtained by distillation (90 °C, 0.3 Torr). Yield: 1.81 g (88%). M.P.: 85 °C. ^{1}H NMR (400 MHz, C_6D_6) δ (ppm): 4.08 (q, J = 7.0 Hz, 4H), 3.11 (hept, J = 6.9 Hz, 2H), 1.29 (d, J = 6.8 Hz, 12H), 1.12 (t, J = 7.1 Hz, 6H). ^{13}C NMR (101 MHz, C_6D_6) δ (ppm): 168.0, 71.3, 36.1, 22.2, 16.0. Anal. Found (Calcd for $C_{12}H_{24}N_2O_2S_2Sn$): C, 35.14 (35.05); H, 5.92 (5.88); N, 6.54 (6.81); S, 15.07 (15.60). HR-MS: $[M]^+$ Found (Calcd for $C_{12}H_{24}N_2O_2S_2Sn$): 412.0296 (412.0301). FT-IR (KBr, cm^{-1}): 2967 (m), 2931 (w), 2898 (w), 2869 (w), 1561 (m), 1552 (m), 1464 (m), 1452 (m), 1443 (m), 1381 (s), 1361 (m), 1308 (w), 1294 (w), 1250 (w), 1197 (w), 1167 (w), 1149 (w), 1115 (w), 1089 (w), 1041 (s), 996 (s), 879 (s), 838 (m), 829 (m), 783 (w), 705 (w), 680 (w), 620 (w), 560 (m).

Crystallographic Analysis. Single crystals of **5** and **7** were grown in saturated toluene at room temperature. Reflection data were collected using a Bruker SMART Apex II-CCD area detector diffractometer with graphite-monochromatized Mo−Kα radiation (λ = 0.71073 Å). The hemisphere of the reflection data was collected as ω-scan frames at 0.3° per frame and an exposure time of 10 s/frame. The cell parameters were determined and refined using the SMART program.[59] Data reduction was performed using SAINT software.[60] The data were corrected for Lorentz and polarization effects. An empirical absorption correction was applied using SADABS software.[61] The structures of the complexes were solved using direct methods and refined by full-matrix least-squares methods using the SHELXTL software package with anisotropic thermal parameters for all non-hydrogen atoms.[62] Cambridge Crystallographic Data Centre (CCDC) files 2342107 and 2342108 for complexes **5** and **7** contain the supplementary crystallographic data for this paper. The data were obtained free of charge from the CCDC (www.ccdc.cam.ac.uk/data_request/cif).

CONCLUSIONS

A series of homoleptic Ge and Sn complexes **1**−**8** containing newly created *N*-alkoxy thioamide ligands were synthesized and characterized as potential single-source precursors of group IV metal chalcogenide materials. The crystallized compounds **5** and **7** were found to be monomers with distorted seesaw geometry. Each molecule forms two κ^2-*O*,*S*-chelating structures as five-membered rings with the corresponding ligands. The thermal stability and volatility of complexes **1**−**8** were evaluated by TG analysis. The curves for the series of Ge compounds showed a single-step weight loss, and the Sn complexes showed multistep weight loss. Among these synthesized complexes, **3** and **7** with the bdpaS ligand showed the lowest residual amounts. In summary, all complexes are expected to be useful single precursors for Ge or Sn chalcogenide materials.

ASSOCIATED CONTENT

Supporting Information

The Supporting Information is available free of charge at https://pubs.acs.org/doi/10.1021/acsomega.4c03019.

NMR and FT-IR spectra of complexes **1**−**8** and data collection parameters for complexes **5** and **7** (PDF)

AUTHOR INFORMATION

Corresponding Author

Taek-Mo Chung − *Thin Film Materials Research Center, Korea Research Institute of Chemical Technology (KRICT), Daejeon 34114, Republic of Korea; Department of Chemical Convergence Materials, University of Science and Technology (UST), Daejeon 34113, Republic of Korea;* orcid.org/0000-0002-5169-2671; Email: tmchung@krict.re.kr

Authors

Heenang Choi − *Thin Film Materials Research Center, Korea Research Institute of Chemical Technology (KRICT), Daejeon 34114, Republic of Korea; Department of Chemistry, Sungkyunkwan University (SKKU), Suwon-si, Gyeonggi-do 16419, Republic of Korea*

Young Eun Song − *Thin Film Materials Research Center, Korea Research Institute of Chemical Technology (KRICT), Daejeon 34114, Republic of Korea; Department of Chemical Convergence Materials, University of Science and Technology (UST), Daejeon 34113, Republic of Korea*

Dongseong Park − *Thin Film Materials Research Center, Korea Research Institute of Chemical Technology (KRICT), Daejeon 34114, Republic of Korea*

Chanwoo Park − *Thin Film Materials Research Center, Korea Research Institute of Chemical Technology (KRICT), Daejeon 34114, Republic of Korea*

Bo Keun Park − *Thin Film Materials Research Center, Korea Research Institute of Chemical Technology (KRICT), Daejeon 34114, Republic of Korea; Department of Chemical Convergence Materials, University of Science and Technology (UST), Daejeon 34113, Republic of Korea;* orcid.org/0000-0002-4066-0500

Seung Uk Son − *Department of Chemistry, Sungkyunkwan University (SKKU), Suwon-si, Gyeonggi-do 16419, Republic of Korea;* orcid.org/0000-0002-4779-9302

Jongsun Lim − *Thin Film Materials Research Center, Korea Research Institute of Chemical Technology (KRICT), Daejeon 34114, Republic of Korea*

Complete contact information is available at: https://pubs.acs.org/10.1021/acsomega.4c03019

Notes

The authors declare no competing financial interest.

ACKNOWLEDGMENTS

We gratefully acknowledge the financial support from the Development of Smart Chemical Materials for IoT Devices Project (KS2421-10) through the Korea Research Institute of Chemical Technology.

REFERENCES

(1) Xia, F.; Mueller, T.; Lin, Y.-M.; Valdes-Garcia, A.; Avouris, P. Ultrafast Graphene Photodetector. *Nat. Nanotechnol.* **2009**, *4*, 839−843.

(2) Sun, Z.; Hasan, T.; Torrisi, F.; Popa, D.; Privitera, G.; Wang, F.; Bonaccorso, F.; Basko, D. M.; Ferrari, A. C. Graphene Mode-Locked Ultrafast Laser. *ACS Nano* **2010**, *4*, 803−810.

(3) Bae, S.; Kim, H.; Lee, Y.; Xu, X.; Park, J. S.; Zheng, Y.; Balakrishnan, J.; Lei, T.; Kim, H. R.; Song, Y. I.; et al. Roll-to-Roll Production of 30-Inch Graphene Films for Transparent Electrodes. *Nat. Nanotechnol.* **2010**, *5*, 574−578.

(4) Liu, M.; Yin, X.; Ulin-Avila, E.; Geng, B.; Zentgraf, T.; Ju, L.; Wang, F.; Zhang, X. A Graphene-Based Broadband Optical Modulator. *Nature* **2011**, *474*, 64−67.
(5) Butler, S. Z.; Hollen, S. M.; Cao, L.; Cui, Y.; Gupta, J. A.; Gutiérrez, H. R.; Heinz, T. F.; Hong, S. S.; Huang, J.; Ismach, A. F.; et al. Progress, Challenges, and Opportunities in Two-Dimensional Materials Beyond Graphene. *ACS Nano* **2013**, *7*, 2898−2926.
(6) Ulaganathan, R. K.; Lu, Y.-Y.; Kuo, C.-J.; Tamalampudi, S. R.; Sankar, R.; Boopathi, K. M.; Anand, A.; Yadav, K.; Mathew, R. J.; Liu, C.-R.; Chou, F. C.; Chen, Y.-T. High Photosensitivity and Broad Spectral Response of Multi-layered Germanium Sulfide Transistors. *Nanoscale* **2016**, *8*, 2284−2292.
(7) Yuan, H.; Liu, X.; Afshinmanesh, F.; Li, W.; Xu, G.; Sun, J.; Lian, B.; Curto, A. G.; Ye, G.; Hikita, Y.; et al. Polarization-Sensitive Broadband Photodetector Using a Black Phosphorus Vertical P-N Junction. *Nat. Nanotechnol.* **2015**, *10*, 707−713.
(8) Xia, F.; Wang, H.; Jia, Y. Rediscovering Black Phosphorus as an Anisotropic Layered Material for Optoelectronics and Electronics. *Nat. Commun.* **2014**, *5*, No. 4458.
(9) Wang, X.; Jones, A. M.; Seyler, K. L.; Tran, V.; Jia, Y.; Zhao, H.; Wang, H.; Yang, L.; Xu, X.; Xia, F. Highly Anisotropic and Robust Excitons in Monolayer Black Phosphorus. *Nat. Nanotechnol.* **2015**, *10*, 517−521.
(10) Shi, G.; Kioupakis, E. Anisotropic Spin Transport and Strong Visible-Light Absorbance in Few-Layer SnSe and GeSe. *Nano Lett.* **2015**, *15*, 6926−6931.
(11) Mannix, A. J.; Zhou, X. F.; Kiraly, B.; Wood, J. D.; Alducin, D.; Myers, B. D.; Liu, X. L.; Fisher, B. L.; Santiago, U.; Guest, J. R.; et al. Synthesis of Borophenes: Anisotropic, Two-Dimensional Boron Polymorphs. *Science* **2015**, *350*, 1513−1516.
(12) Lorchat, E.; Froehlicher, G.; Berciaud, S. Splitting of Interlayer Shear Modes and Photon Energy Dependent Anisotropic Raman Response in *N*-Layer $ReSe_2$ and ReS_2. *ACS Nano* **2016**, *10*, 2752−2760.
(13) Antunez, P. D.; Buckley, J. J.; Brutchey, R. L. Tin and Germanium Monochalcogenide IV−VI Semiconductor Nanocrystals for Use in Solar Cells. *Nanoscale* **2011**, *3*, 2399−2411.
(14) Li, C.; Huang, L.; Snigdha, G. P.; Yu, Y.; Cao, L. Role of Boundary Layer Diffusion in Vapor Deposition Growth of Chalcogenide Nanosheets: The Case of GeS. *ACS Nano* **2012**, *6*, 8868−8877.
(15) Xue, D. J.; Tan, J.; Hu, J. S.; Hu, W.; Guo, Y. G.; Wan, L. J. Anisotropic Photoresponse Properties of Single Micrometer-Sized GeSe Nanosheet. *Adv. Mater.* **2012**, *24*, 4528−4533.
(16) Kim, J. Y.; George, S. M. Tin Monosulfide Thin Films Grown by Atomic Layer Deposition Using Tin 2,4-Pentanedionate and Hydrogen Sulfide. *J. Phys. Chem. C* **2010**, *114*, 17597−17603.
(17) Sinsermsuksakul, P.; Hartman, K.; Kim, S. B.; Heo, J.; Sun, L.; Park, H. H.; Chakraborty, R.; Buonassisi, T.; Gordon, R. G. Enhancing the Efficiency of SnS Solar Cells via Band-Offset Engineering with a Zinc Oxysulfide Buffer Layer. *Appl. Phys. Lett.* **2013**, *102*, No. 053901.
(18) Deng, Z.; Cao, D.; He, J.; Lin, S.; Lindsay, S. M.; Liu, Y. Solution Synthesis of Ultrathin Single-Crystalline SnS Nanoribbons for Photodetectors via Phase Transition and Surface Processing. *ACS Nano* **2012**, *6*, 6197−6207.
(19) Mathews, N. R. Electrodeposited Tin Selenide Thin Films for Photovoltaic Applications. *Sol. Energy* **2012**, *86*, 1010−1016.
(20) Li, L.; Chen, Z.; Hu, Y.; Wang, X.; Zhang, T.; Chen, W.; Wang, Q. Single-Layer Single-Crystalline SnSe Nanosheets. *J. Am. Chem. Soc.* **2013**, *135*, 1213−1216.
(21) Nörenberg, T.; Álvarez-Pérez, G.; Obst, M.; Wehmeier, L.; Hempel, F.; Klopf, J. M.; Nikitin, A. Y.; Kehr, S. C.; Eng, L. M.; Alonso-González, P.; de Oliveira, T. V. A. G. Germanium Monosulfide as a Natural Platform for Highly Anisotropic THz Polaritons. *ACS Nano* **2022**, *16*, 20174−20185.
(22) Anne, M. L.; Keirsse, J.; Nazabal, V.; Hyodo, K.; Inoue, S.; Boussard-Pledel, C.; Lhermite, H.; Charrier, J.; Yanakata, K.; Loreal, O.; Le Person, J.; Colas, F.; Compère, C.; Bureau, B. Chalcogenide Glass Optical Waveguides for Infrared Biosensing. *Sensors* **2009**, *9*, 7398−7411.
(23) Im, H. S.; Myung, Y.; Park, K.; Jung, C. S.; Lim, Y. R.; Jang, D. M.; Park, J. Ternary Alloy Nanocrystals of Tin and Germanium Chalcogenides. *RSC Adv.* **2014**, *4*, 15695−15701.
(24) Mishra, N.; Makov, G. Ab initio study of intrinsic point defects in germanium sulfide. *J. Alloys Compd.* **2022**, *914*, No. 165389.
(25) Li, F.; Liu, X.; Wang, Y.; Li, Y. Germanium Monosulfide Monolayer: A Novel Two-Dimensional Semiconductor with a High Carrier Mobility. *J. Mater. Chem. C* **2016**, *4*, 2155−2159.
(26) Kim, H. S.; Jung, E. A.; Han, S. H.; Han, J. H.; Park, B. K.; Kim, C. G.; Chung, T.-M. Germanium Compounds Containing Ge═E Double Bonds (E = S, Se, Te) as Single-Source Precursors for Germanium Chalcogenide Materials. *Inorg. Chem.* **2017**, *56*, 4084−4092.
(27) Cho, Y. J.; Im, H. S.; Myung, Y.; Kim, C. H.; Kim, H. S.; Back, S. H.; Lim, Y. R.; Jung, C. S.; Jang, D. M.; Park, J.; Cha, E. H.; Choo, S. H.; Song, M. S.; Cho, W. I. Germanium Sulfide (II and IV) Nanoparticles for Enhanced Performance of Lithium Ion Batteries. *Chem. Commun.* **2013**, *49*, 4661−4663.
(28) Zhao, P.; Yang, H.; Li, J.; Jin, H.; Wei, W.; Yu, L.; Huang, B.; Dai, Y. Design of new photovoltaic systems based on two-dimensional group-IV monochalcogenides for high performance solar cells. *J. Mater. Chem. A* **2017**, *5*, 24145−24152.
(29) Yang, M.; Cao, S.; You, Q.; Shi, L.-B.; Qian, P. Intrinsic Carrier Mobility of Monolayer GeS and GeSe: First-Principles Calculation. *Phys. E* **2020**, *118*, No. 113877, DOI: 10.1016/j.physe.2019.113877.
(30) Albers, W.; Haas, C.; van der Maesen, F. The Preparation and the Electrical and Optical Properties of SnS Crystals. *J. Phys. Chem. Solids* **1960**, *15*, 306−310.
(31) Mathews, N. R.; Anaya, H. B. M.; Cortes-Jacome, M. A.; Angeles-Chavez, C.; Toledo-Antonio, J. A. Tin Sulfide Thin Films by Pulse Electrodeposition: Structural, Morphological, and Optical Properties. *J. Electrochem. Soc.* **2010**, *157*, H337−H341.
(32) Burton, L. A.; Colombara, D.; Abellon, R. D.; Grozema, F. C.; Peter, L. M.; Savenije, T. J.; Dennler, G.; Walsh, A. Synthesis, Characterization, and Electronic Structure of Single-Crystal SnS, Sn_2S_3 and SnS_2. *Chem. Mater.* **2013**, *25*, 4908−4916.
(33) Wangperawong, A.; Hsu, P.-C.; Yee, Y.; Herron, S.-M.; Clemens, B.-M.; Cui, Y.; Bent, S. F. Bifacial Solar Cell with SnS Absorber by Vapor Transport Deposition. *Appl. Phys. Lett.* **2014**, *105*, No. 173904.
(34) Ran, F. Y.; Xiao, Z.; Toda, Y.; Hiramatsu, H.; Hosono, H.; Kamiya, T. n-Type Conversion of SnS by Isovalent Ion Substitution: Geometrical Doping as a New Doping Route. *Sci. Rep.* **2015**, *5*, No. 10428.
(35) Ramakrishna Reddy, K. T.; Koteswara Reddy, N.; Miles, R. W. Photovoltaic Properties of SnS Based Solar Cells. *Sol. Energy Mater. Sol. Cells* **2006**, *90*, 3041−3046.
(36) Skelton, J. M.; Burton, L. A.; Oba, F.; Walsh, A. Chemical and Lattice Stability of the Tin Sulfides. *J. Phys. Chem. C* **2017**, *121*, 6446−6454.
(37) Vaughn, D. D.; Patel, R. J.; Hickner, M. A.; Schaak, R. E. Single-Crystal Colloidal Nanosheets of GeS and GeSe. *J. Am. Chem. Soc.* **2010**, *132*, 15170−15172.
(38) Xu, J.; Almeida, R. M. Preparation and Characterization of Germanium Sulfide Based Sol-Gel Planar Waveguides. *J. Sol-Gel Sci. Technol.* **2000**, *19*, 243−248.
(39) Murugesan, S.; Kearns, P.; Stevenson, K. J. Electrochemical Deposition of Germanium Sulfide from Room-Temperature Ionic Liquids and Subsequent Ag Doping in an Aqueous Solution. *Langmuir* **2012**, *28*, 5513−5517.
(40) Kim, S. B.; Sinsermsuksakul, P.; Hock, A. S.; Pike, R. D.; Gordon, R. G. Synthesis of N-Heterocyclic Stannylene (Sn(II)) and Germylene (Ge(II)) and a Sn(II) Amidinate and Their Application as Precursors for Atomic Layer Deposition. *Chem. Mater.* **2014**, *26*, 3065−3073.
(41) Whitham, P. J.; Strommen, D. P.; Lundell, S.; Lau, L. D.; Rodriguez, R. GeS_2 and $GeSe_2$ PECVD from $GeCl_4$ and Various

Chalcogenide Precursors. *Plasma Chem. Plasma Process.* **2014**, *34*, 755−766.
(42) Miles, R. W.; Ogah, O. E.; Zoppi, G.; Forbes, I. Thermally Evaporated Thin Films of SnS for Application in Solar Cell Devices. *Thin Solid Films* **2009**, *517*, 4702−4705.
(43) Sinsermsuksakul, P.; Heo, J.; Noh, W.; Hock, A. S.; Gordon, R. G. Atomic Layer Deposition of Tin Monosulfide Thin Films. *Adv. Energy Mater.* **2011**, *1*, 1116−1125.
(44) Robinson, F.; Sethi, V.; de Groot, C. H. K.; Hector, A. L.; Huang, R.; Reid, G. Low-Pressure CVD of GeE (E = Te, Se, S) Thin Films from Alkylgermanium Chalcogenolate Precursors and Effect of Deposition Temperature on the Thermoelectric Performance of GeTe. *ACS Appl. Mater. Interfaces* **2021**, *13*, 47773−47783.
(45) Marchand, P.; Carmalt, C. J. Molecular Precursor Approach to Metal Oxide and Pnictide Thin Films. *Coord. Chem. Rev.* **2013**, *257*, 3202−3221.
(46) Malik, M. A.; Afzaal, M.; O'Brien, P. Precursor Chemistry for Main Group Elements in Semiconducting Materials. *Chem. Rev.* **2010**, *110*, 4417−4446.
(47) Bade, B. P.; Garje, S. S.; Niwate, Y. S.; Afzaal, M.; O'Brien, P. Tribenzyltin(IV)chloride Thiosemicarbazones: Novel Single Source Precursors for Growth of SnS Thin Films. *Chem. Vap. Deposition* **2008**, *14*, 292−295.
(48) Ramasamy, K.; Kuznetsov, V. L.; Gopal, K.; Malik, M. A.; Raftery, J.; Edwards, P. P.; O'Brien, P. Organotin Dithiocarbamates: Single-Source Precursors for Tin Sulfide Thin Films by Aerosol-Assisted Chemical Vapor Deposition (AACVD). *Chem. Mater.* **2013**, *25*, 266−276.
(49) Catherall, A. L.; Harris, S.; Hill, M. S.; Johnson, A. L.; Mahon, M. F. Deposition of SnS Thin Films from Sn(II) Thioamidate Precursors. *Cryst. Growth Des.* **2017**, *17*, 5544−5551.
(50) Ahmet, I. Y.; Guc, M.; Sánchez, Y.; Neuschitzer, M.; Izquierdo-Roca, V.; Saucedo, E.; Johnson, A. L. Evaluation of AA-CVD Deposited Phase Pure Polymorphs of SnS for Thin Films Solar Cells. *RSC Adv.* **2019**, *9*, 14899−14909.
(51) Ahmet, I. Y.; Hill, M. S.; Raithby, P. R.; Johnson, A. L. Tin Guanidinato Complexes: Oxidative Control of Sn, SnS, SnSe and SnTe Thin Film Deposition. *Dalton Trans.* **2018**, *47*, 5031−5048.
(52) George, S. M.; Nam, J. H.; Lee, G. Y.; Han, J. H.; Park, B. K.; Kim, C. G.; Jeon, D. J.; Chung, T.-M. *N*-Alkoxy Carboxamide Stabilized Tin(II) and Germanium(II) Complexes for Thin-Film Applications. *Eur. J. Inorg. Chem.* **2016**, *2016*, 5539−5546.
(53) Yang, D.; Liu, G.-J.; Jiao, Z.-G.; Zhang, D.-W.; Luo, Z.; Song, K.-S.; Chen, M.-Q. Disulfide Bond Creates a Small Connecting Loop in Aminoxy Peptide Backbone. *Chem. Eur. J.* **2008**, *14*, 10297−10302.
(54) Gynane, M. J. S.; Harris, D. H.; Lappert, M. F.; Power, P. P.; Rivière, P.; Rivière-Baudet, M. Subvalent Group 4B metal alkyls and amides. Part 5. The synthesis and physical properties of thermally stable amides of germanium(II), tin(II), and lead(II). *J. Chem. Soc., Dalton Trans.* **1977**, 2004−2009.
(55) Nyquist, R. Thiols, Sulfides and Disulfides, Alkanethiols, and Alkanedithiols (S-H Stretching). In *Interpreting Infrared: Raman, and Nuclear Magnetic Resonance Spectra*, 2001; Vol. *2*, pp 65−83.
(56) Jensen, W. P.; Palenik, G. J.; Tiekink, E. R. T. Bond Valence Sums in Coordination Chemistry. Sn(II), Sn (III), and Sn(IV) Complexes Containing Sn-S and/or Sn-N Bonds. *Polyhedron* **2001**, *20*, 2137−2143.
(57) Harris, D. H.; Lappert, M. F. Monomeric, Volatile Bivalent Amides of Group IV_B elements, $M(NR_2^1)_2$ and $M(NR^1R^2)_2$ (M = Ge, Sn, or Pb; R^1=Me_3Si, R2 = Me_3C). *J. Chem. Soc. Chem. Commun.* **1974**, *21*, 895−896.
(58) Gynane, M. J. S.; Harris, D. H.; Lappert, M. F.; Power, P. P.; Rivière, P.; Rivière-Baudet, M. Subvalent Group 4B Metal Alkyls and Amides. Part 5. The Synthesis and Physical Properties of Thermally Stable Amides of Germanium(II), Tin(II), and Lead(II). *J. Chem. Soc., Dalton Trans.* **1977**, *20*, 2004−2009.
(59) SMART. *Data Collection Software*. Version 5.0, Bruker AXS, Inc.: Madison, WI, 1998.
(60) SMART. *Data Integration Software*. Version 5.0, Bruker AXS, Inc.: Madison, WI, 1998.
(61) Sheldrick, G. M. *SADABS, Program for Absorption Correction with the Bruker SMART System*; Universität Göttingen: Germany, 1996.
(62) Sheldrick, G. M. *SHELXL-93: Program for the Refinement of Crystal Structures*; Universität Göttingen: Germany, 1996.

https://doi.org/10.1021/acsomega.4c03019
ACS Omega 2024, 9, 28707−28714